#18748

# Simulation and comparison of infra-red sensors for automotive applications

T. Meitzler,[a] E. Sohn,[a] R. Karlsen,[a] G. Gerhart,[a] and S. Lakshmanan[b]

[a] US Army Tank-Automotive and Armaments Command
AMSTA-TR-S
Warren, MI, 48397-5000
E-mail: meitzlet@TACOM-emh165.army.mil; Phone:(810)574-7530

[b] Department of Electrical and Computer Engineering, University of Michigan-Dearborn
Dearborn, MI 48128-1491

## ABSTRACT

This paper presents a simulation and comparison of two different infrared (IR) imaging systems in terms of their use in automotive collision avoidance and vision enhancement applications. The first half of this study concerns the simulations of a "cooled" shortwave focal plane array infrared imaging system, and an "uncooled" focal plane array infrared imaging system. This is done using the United States Army's Tank-Automotive Research Development and Engineering Center's (TARDEC) Thermal Image Model - (TTIM). Visual images of automobiles as seen through a forward looking infrared sensor are generated, by using TTIM, under a variety of viewing range, and rain conditions. The second half of the study focuses on a comparison between the two simulated sensors. This comparison is undertaken from the standpoint of the ability of a human observer to detect potential (collision) targets, when looking through the two different sensors. A measure of the target's detectability is derived for each sensor by using the TARDEC's Visual Model (TVM). The authors found the uncooled pyroelectric FPA to give excellent imagery and, combined with the advantages of the 7.5-13.5 band in the atmosphere and the higher blackbody exitance in the 7.5-13.5 band, the 7.5-13.5 uncooled sensor is therefore the better choice for imaging through numerous atmospheric conditions compared to the 3.4-5.5 cooled sensor.

**Keywords**: infrared sensors, pyroelectric sensors, simulation, atmospheric bandpass

## 2. INTRODUCTION

Collision avoidance and vision enhancement systems are seen as an integral part of the next generation of active automotive safety devices[1, 2]. Automotive manufacturers are evaluating a variety of imaging sensors for their usefulness in such systems [1]. One potential application for automobiles is a driver's vision-enhancement system[11]. This use of night vision sensors as a safety feature would allow drivers to see objects at a distance of about 1500 ft., far beyond the range of headlights. Obstacles in the drivers peripheral visual field of view could be seen and recognized much sooner. Sensors that operate at wavelengths close to the eletromagnetic frequency band of human vision (such as video cameras) provide images that have good spatial resolution. However, the quality of the images (in terms of relative contrast and spatial resolution) acquired by such a camera degrades drastically under conditions of poor light, rain, fog, smoke, etc.. One way to overcome such poor conditions is to choose an imaging sensor that operates at longer (than visual) wavelengths. The relative contrast in images acquired from such sensors does not degrade as drastically under poor visibility conditions. However, this characteristic comes at a cost; the spatial resolution of the image provided by such sensors is less than that provided by a video camera.

# Report Documentation Page

*Form Approved*
*OMB No. 0704-0188*



| 1. REPORT DATE | 2. REPORT TYPE | 3. DATES COVERED |
|---|---|---|
| **19 APR 1995** | **N/A** | **-** |

| 4. TITLE AND SUBTITLE | 5a. CONTRACT NUMBER |
|---|---|
| **Simulation and comparison of infrared sensors for automotive applications** | 5b. GRANT NUMBER |
| | 5c. PROGRAM ELEMENT NUMBER |

| 6. AUTHOR(S) | 5d. PROJECT NUMBER |
|---|---|
| **Thomas J. Meitzler; Euijung Sohn; Robert E. Karlsen; Grant R. Gerhart; Sridhar Lakshmanan** | 5e. TASK NUMBER |
| | 5f. WORK UNIT NUMBER |

| 7. PERFORMING ORGANIZATION NAME(S) AND ADDRESS(ES) | 8. PERFORMING ORGANIZATION REPORT NUMBER |
|---|---|
| **US Army RDECOM-TARDEC 6501 E 11 Mile Rd Warren, MI 48397-5000** | **18748** |

| 9. SPONSORING/MONITORING AGENCY NAME(S) AND ADDRESS(ES) | 10. SPONSOR/MONITOR'S ACRONYM(S) |
|---|---|
| | **TACOM/TARDEC** |
| | 11. SPONSOR/MONITOR'S REPORT NUMBER(S) |
| | **18748** |

12. DISTRIBUTION/AVAILABILITY STATEMENT

**Approved for public release, distribution unlimited**

13. SUPPLEMENTARY NOTES

**Pub. in Proc. SPIE Vol.2470,p. 38-46, Infrared Imaging Systems: Design, Analysis, Modeling, and Testing VI, Gerald C. Holst; Ed.**

14. ABSTRACT

15. SUBJECT TERMS

| 16. SECURITY CLASSIFICATION OF: | | | 17. LIMITATION OF ABSTRACT | 18. NUMBER OF PAGES | 19a. NAME OF RESPONSIBLE PERSON |
|---|---|---|---|---|---|
| a. REPORT | b. ABSTRACT | c. THIS PAGE | | | |
| **unclassified** | **unclassified** | **unclassified** | **SAR** | **9** | |

Passive infrared sensors operate at a wavelength slightly longer that the visual spectrum. (The visual spectrum is between 0.4 and 0.7 microns, and the commonly used portions of the infrared spectrum are in the atmospheric "windows" that reside between 0.7 and 14 microns). Hence the IR sensors perform better than a video camera (in terms of relative contrast) when the visibility conditions are poor. Also, since their wavelength of operation is only slightly longer, the quality of the image provided by an infrared sensor is comparable to that of a video camera (in terms of spatial resolution). As a result, infrared sensors have much potential for use in automotive collision avoidance systems [1, 3].

Of all the different types of infrared detector technologies there are two state-of-the-art infrared detectors considered in this paper, that offer benefcial alternatives when it comes to an infrared sensor system for automotive and surveillance applications. The first alternative is based on a cooled focal plane array (FPA) of CMOS PtSi infrared detectors that operate in the 3.4 -5.5μm wavelength band. The second alternative is based on a staring uncooled barium strontium titanate (BST) FPA of ceramic sensors that operate in the 7.5 - 13.5 micron wavelength band. Under clear atmospheric conditions and at ranges less than 500 meters the 3.4-5.5 micron systems generate images with less contrast than the 7.5-13.5 micron system. Dual-band field data show that the 3.4-5.5 band systems present more contrast between temperature extremes whereas the 7.5-13.5 band systems show more detail in the overall picture.

The TACOM Thermal Image Model (TTIM) is a computer model that simulates the appearance of a thermal scene as seen through an IR imaging system [6]. TTIM can simulate the sampling effects of the older single detector scanning systems, as well as more modern systems that use focal plane staring arrays. TTIM can also model image intensifiers. A typical TTIM simulation incorporates the image degrading effects of several possible atmospheric conditions, by using LOWTRAN - a computer model of the effects of atmosphere conditions on thermal radiation that was developed at the United States Air Force's Geophysics Laboratory. A particularly attractive feature of TTIM is that is produces a simulated image for the viewer, not a set of numbers as some of the other simulations do. We refer the reader to Fig. 1 for schematic representation of TTIM.

**Figure 1: Schematic representation of TTIM**

In the first half of this paper we use TTIM to simulate the cooled and uncooled infrared (IR) imaging systems, and compare their performance from the standpoint of automotive applications. Analogous comparisons exist in the current literature [4, 5]. However, it is our opinion that such studies are not applicable for the situation at hand. TTIM and TVM *together* allow the comparison of the performance of the two IR systems in terms of how good the quality of their images is for subsequent human perception/interpretation. The existing studies do not allow such comparisons.

The comparison of system performance leads us to the second half of this paper. Given that we have two images of the same scene, captured by using the two different infra-red systems, we use TVM to assess which of the two is "better". TVM is a computational model of the human visual system [7]. Within the functional area of signature analysis, the unclassified model consists of two parts: early human vision modeling and signal detection. The early vision part of the model itself is made up of two basic parts, the first part is a color separation module, and the second part is a spatial frequency decomposition module. The color separation module is akin to the human visual system. The spatial frequency decomposition system is based on a Gaussian-Laplacian pyramid framework. Such pyramids are special cases of wavelet pyramids, and they represent a reasonable model of spatio-frequency channels in early human vision [8]. We refer the reader to Fig. 2 for a schematic representation of TVM.

**Figure 2: Schematic representation of TVM**

## 3. SIMULATION OF INFRA-RED SENSORS

This section presents the simulation of cooled and uncooled infrared imaging systems using TTIM. Specifically, we use as input to TTIM actual thermal images of commercial vehicles in a typical road scene and then resample the image using TTIM. The initial infrared images were taken at TARDEC with the pyroelectric sensor from Texas Instruments (TI). We present examples of how the rain affects the quality of the sensor displayed image. Throughout this paper "target" shall be synonomous with the "object-of-interest" in the scene and "no-target" shall mean the image with the "object-of-interest removed."

We see this type of simulation as a substantial first step, and as providing a means to comprehensively evaluate and compare the sensor systems for commercial use in the future. Our ability to simulate the sensors provides a means for exactly repeating imaging experiments and measurements, something that is difficult to achieve in field trials. Also based on our experience, the ability to simulate the sensors provides us with the ability to exercise precise control over the imaging conditions. In the cooled infrared systems, for example, it is important to provide proper temperature shielding during field trials. Otherwise, the quality of the images acquired from the infrared system is badly affected, and it negatively impacts the validity of subsequent comparisons between sensor systems. By simulating cooled infrared systems we can overcome such difficulties.

In Figure 6 we present simulated infrared images of typical commercial vehicles when the viewing distance (the distance between the vehicle and the sensor) is fixed, and the amount of rainfall under which the image is acquired increases. This is done for both the cooled and uncooled cases by inputing into TTIM the thermal image containing the target and no-target image. The images have been resampled according to the specific sensor and then degraded by rain and fog.

## 4. SENSOR COMPARISON

In this section we use TVM to compare the quality of images acquired from the cooled and the uncooled infra-red imaging systems through rain and fog. Then, using TVM we obtain the SNR and a measure of detectability , d', in each of the images for a vehicle of interest. Specifically, we input into TVM the target and no-target images, corresponding to the infra-red systems.

### The TVM Signature Vector

Sampling of image contrast by the human visual system is represented by a series of Gaussian filters that render approximate derivatives of contrast gradient over space [9]. Each filter performs a spatial frequency bandpass operation in one frontal-plane dimension, and low-pass filters the orthogonal dimension. In the case of TVM, these spatial filters are implemented sequentially with a simple five-pixel kernel in each of two orthogonal frontal-plane directions. A set of seven bandpass filters centered at different spatial frequencies and differing by one octave is implemented as a pyramidal hierarchy of filters in which the image input to the next lower filter is obtained as a residual of the operation of the next higher one. TVM applies these seven bandpass filters across three color-opponent channels, each of which is divided into two orientations, giving 42 channel outputs in all. Each of these channel outputs contains a constituent of the original image that represents a different component of the human visual systems's target detection mechanism.

In a manner similar to standard amplitude modulation signal detection, TVM obtains the contrast modulation energy (CME) of a single channel by squaring its amplitude-modulated output, then low-pass filtering the result to obtain an energy-envelope function, as illustrated in Figure 3. TVM iterates this process across the preselected target and background areas within a single channel to obtain the averages and the variances of a channels target and background CME's. The difference between a channel's average target and background CME provides one metric of a channel's contribution to target detection and the difference between target and background CME variances provides a second one as shown in equation (1). A single signature metric of channel output which combines these measures is defined by equations (1), (2) and (3). These equations define the necessary parameters for a single-channel SNR assessment. The noise term includes noise internal to the eye, which is a function of illumination level, and a clutter noise term, which is estimated from the CME background statistics.

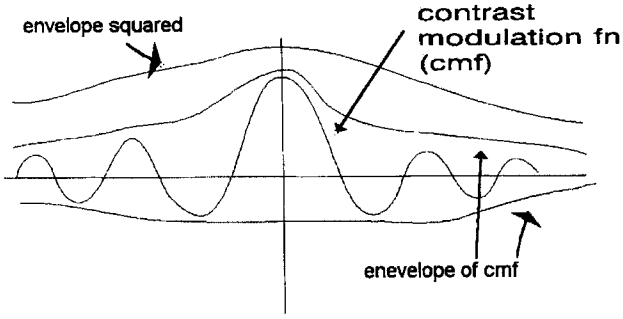


**Figure 3. Extracting the energy envelopes of spatial bandpass filters.** Prior to their combination according to TVM rules, the amplitude-modulated outputs within each of 42 spatial bandpass channels are squared and then low-pass filtered to obtain their contrast modulation energy (CME) envelopes.

$$\Delta Signal = \sqrt{\left|\sigma_{tgt}^2 - \sigma_{bkg}^2\right| + \left|\mu_{tgt} - \mu_{bkg}\right|^2} \quad (1)$$

$$\Delta Signal = \sqrt{\left|Change\ in\ Energy\ Variance\right| + \left|Change\ in\ Energy\right|^2} \quad (2)$$

$$Noise = \sqrt{ICN\ noise\ power + BKG\ noise\ power} \quad (3)$$

The TVM signature vector comprises the 42 single-channel SNR estimates, each of which is weighted in proportion to the relative number of receptive fields of each bandpass-type found in human vision. TVM aggregates these weighted SNR estimates according to the cortical pooling model of Watson [9] in euation (4), which specifies that the density of receptive fields of any spatial bandpass type on the retinal surface is an inverse function of retinal eccentricity from the fovea. The resulting quantity d in equation (5) is the detectability metric derived by TVM. The exponent QSNR in equation (5) is approximately 2, corresponding to an ideal observer model for signal detection theory. As expressed in equation (6), d has a log-linear relationship to d', the TVM output parameter. The parameter d' specifies a human receiver-operator characteristic (ROC) curve from which detectability in terms of p(hit) can be predicted as a function of a given p(fa), and/or a function of an observer's propensity for guessing.

$$SNR_{c,a,f} = \frac{\Delta signal_{c,a,f}}{Noise_{c,a,f}} \quad (4)$$

$$d(\varepsilon) = \sum_{c,a,f} NRF_{c,f}^{QSNR}(\varepsilon) SNR_{c,a,f}^{QSNR} \quad (5)$$

$$d'(\varepsilon) = \psi_1 d(\varepsilon)^{\psi_2} \quad (6)$$

The detectability measure, d', obtained from TVM is proportional to the SNR between the vehicle of interest and the background (as explained in Fig. 2). Next in Figure 4 we plot the highest SNR of all frequency channels as a function of the rain rate. The curve in Figure 4 with the higher whole image SNR is that of the uncooled pyroelectric FPA.

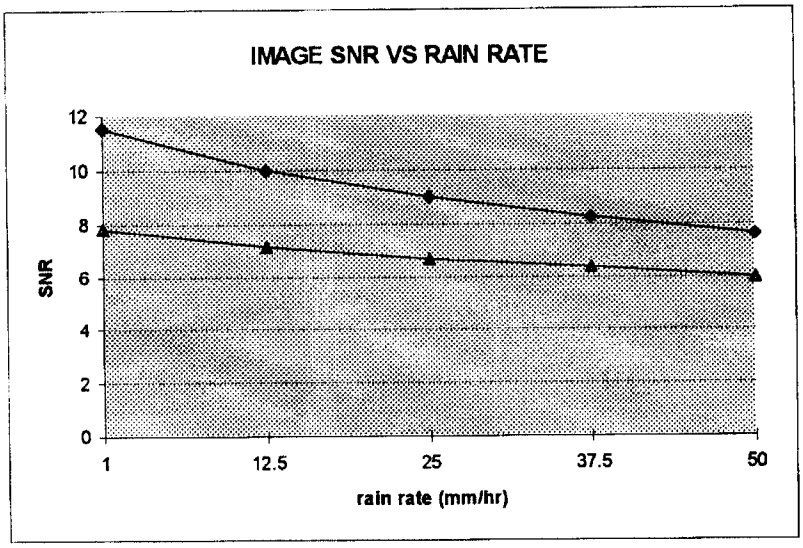


**Figure 4: Image SNR vs Rain Rate**

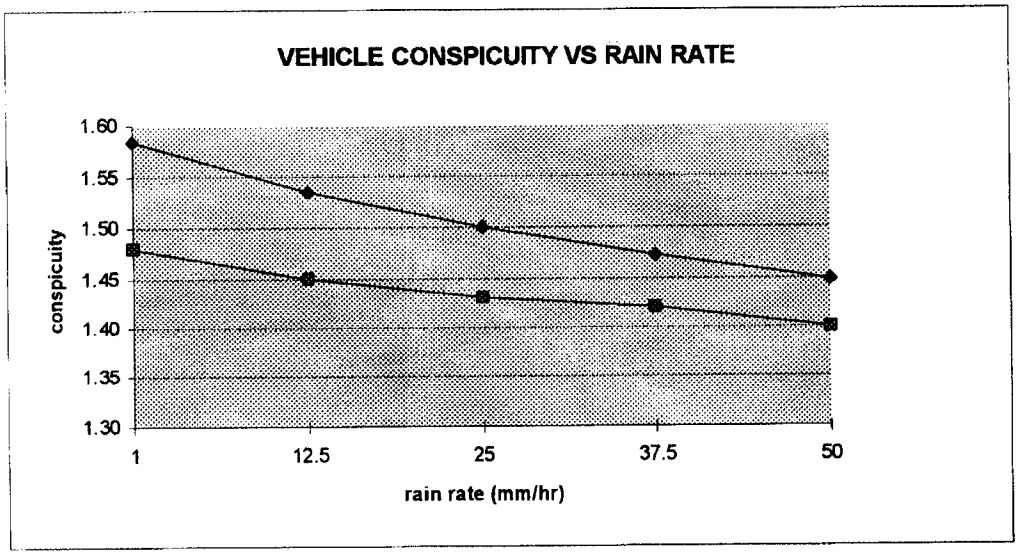


**Figure 5: Conspicuity vs Rain Rate**

Figure 5 shows the predicted conspicuities of the vehicles when viewed through the sensors and atmosphere. The two curves in Figure 5 are the detectabilities of the target vehicle as predicted by the visual model. Predictions based on different metrics for background clutter will be the subject of a future paper. For this particular case, the conspicuity of the target as seen through the uncooled 7.5-13.5 band has the higher predicted conspicuity. In figure 6, the computer simulated images are shown for the uncooled and cooled camera. The top row is the clear case with and without the object of interest, which is the car at the center of the picture. The range for all the pictures is 70 meters. The second row is for the case of fog. As one goes down the columns of images, the rain rate is 1, 12.5, 25, 37.5 and 50 mm/hr respectively. The images show that the longwave uncooled camera provides a higher contrast picture under all conditions. Given two simulated infrared sensor images from TTIM of the same scene, an object of interest, and the background, we use TVM to compute a SNR for the whole image and a measure of detectability d' for the object of interest in each of the images. The image with the higher SNR has a greater contrast and is easier to interpret. The object of interest in a scene with the higher d' has a higher conspicuity and is therefore easier to see.

**Figure 6: Uncooled 7.5-13.5 vs cooled 3.4-4.5 camera**

## 5. CONCLUSIONS

In this paper we provided a simulation of and a comparison between cooled and uncooled infrared imaging systems. This was done with a view towards using such systems for automotive collision avoidance applications. Using TTIM, we successfully simulated both infrared imaging systems. We provided simulated images as seen through these sensors when the viewing distance is constant and when the amount of rainfall under which the images are acquired increases. In a previous paper [10] the contrast scaling was based on a pooling of all the images for both sensors. In this paper, the authors did the scaling of contrast manually per sensor type. This gave results that are in better agreement with field data and sensor performance. The 7.5-13.5 band has more background radiance in the scenes which tends to add more grey to the image as rain rate increases, whereas, the 3.4-5.5 band gets greyer with increasing rain rate primarily due to the radiance loss due to scattering. These model predictions are consistent with infrared field images of test patterns, through both bands, in the rain. Scattering losses are compounded by the shape of the Planck blackbody exitance distribution. The shape of the blackbody curves at a temperature of 300K show that the 7.5-13.5 band has almost a factor of 2 more exitance. Using the TVM we compare the two sensors. In each of the spatial frequency channels found in early vision among humans, we obtained a measure of detectability for an object and background of interest.

We ploted the SNR versus rain rate for both the sensors, and obtained the variation in the SNR as the amount of rain fall under which the images are acquired increases. Based on the computer simulations the authors performed, our suggestions for a commercial infrared unit for use in collision avoidance or vision enhancement system are as follows, (1) since the 7.5-13.5 band has more exitance than the 3.4-5.5 band, and (2) the transmittance is nearly a factor of 1.5 better in rain the 7.5-13.5 band, (3) coupled with the fact that the uncooled imagery was excellant in quality, we suggest using the 7.5-13.5 band, uncooled pyroelectric sensor. In addition, the unit used for data collection was in fact several years old, and there has since been a 50% increase in the detector sensitivity along with improvements in the detector uniformity and system implimentation.

Sensor comparisons are one aspect of collision avoidance and vision enhancement. There are a number of other human factors and social issues as well associated with the "science of collision avoidance" as pointed out in [2].

## 6. ACKNOWLEDGMENTS

We gratefully appreciate the help of Mr. Sam McKenney and the use of the uncooled pyroelectric sensor from Texas Instruments. The authors are also grateful to Mr. Wendel Watkins of ARL for the use of his images of test patterns taken in the rain.

## 7. REFERENCES


[1] IEEE Micro: Special Issue on Automotive Electronics,Vol. 13, 1993.

[2] R.K. Deering and D.C. Viano, "Critical success factors for crash avoidance countermeasure implementation," Proc. Intl. Congress on Transp. Electronics, pp. 209-214, 1994

[3] S. Klapper, B. Stearns, and C. Wilson, "Low cost infrared technologies make night vision affordable for law enforcement agencies and consumers," Proc. Intl. Congress on Transp. Electronics, pp. 341-345, 1994.

[4] G.A. Findlay, and D.R. Cutten, "Comparison of performance of 3-5 and 8-12 micron infrared system," Applied Optics, Vol. 28, pp. 5029-5037, 1989.

[5] T.W. Tuer, "Thermal imaging systems relative performance: 3-5 vs 8-12 microns," Technical Report, AFL-TR-76-217

[6] C.S. Hall, E.T. Buxton, and T.J. Rogne, TACOM thermal image model version 3.1: technical reference and users guide, OptiMetrics, Inc. Tech. Reort OMI-405, 1993.

[7] G.H. Lindquist, G. Witus, et al., "Target discrimination using computational vision human perception models," Proceedings of the SPIE Conference on Infrared Imaging Systems: Design, Analysis, Modeling and Testing, Vol. 2224, pp. 30-40, 1994.

[8] J. Malik and P. Perona, "Preattentive texture discrimination with early vision mechanisms," J. Op. Soc. Am., Vol. 7, pp. 923-932, 1990.

[9] A.B. Watson, "Detection and recognition of simple spatial forms," NASA Tech Memo No. 84353, National Aeronautics and Space Administration, Moffett Field, CA, 1983.

[10] S. Lakshmanan and T. Meitzler , EJ Sohn, and G. Gerhart., "Simulation and comparison of infrared sensors for automotive collision avoidance," SAE Technical Paper 950471, March 95.

[11] P.W. Kruse, "Thermal imagers move from the military to the marketplace," Photonics Spectra, pp. 103-108, March 1995.